Fluorous Versions of Wilkinson's Catalyst. Activity in Fluorous Hydrogenation of 1-Alkenes and Recycling by Fluorous Biphasic Separation

Bodo Richter,[†] Anthony L. Spek,[‡] Gerard van Koten,[†] and Berth-Jan Deelman*[,§]

Contribution from the Debye Institute, Department of Metal-Mediated Synthesis, Utrecht University, Padualaan 8, 3584 CH Utrecht, The Netherlands, Bijvoet Center for Biomolecular and Structural Chemistry, Utrecht University, Padualaan 8, 3584 CH Utrecht, The Netherlands, and Elf Atochem Vlissingen B.V., P.O. Box 70, 4380 AB Vlissingen, The Netherlands

Received October 4, 1999

Abstract: Two novel fluorous tris(arylphosphine)rhodium(I) chloride complexes RhCl[P{C_6H_4-*p*-$SiMe_2$-$(CH_2)_2C_nF_{2n+1}$}$_3$]$_3$ (**3a**: $n = 6$, **3b**: $n = 8$) being fluorous analogues of Wilkinson's catalyst show high activity in hydrogenation of 1-alkenes under single phase fluorous conditions and can be effectively recycled using the new concept of fluorous biphasic separation. For comparison the *p*-(trimethylsilyl)-substituted derivative RhCl[P(C_6H_4-*p*-$SiMe_3$)$_3$]$_3$ (**3c**) has also been synthesized and the X-ray structure of dimeric [Rh(μ-Cl){P(C_6H_4-*p*-$SiMe_3$)$_3$}$_2$]$_2$ (**4c**) was determined. A comparison of the catalytic activity of the fluorous catalysts and the nonfluorous derivatives under identical conditions revealed a decreasing activity in the order **3c** > **3a** > RhCl-$(PPh_3)_3$ > **3b**. The recycling efficiency of the new catalysts (> 98% for **3b**) is much better than expected on the basis of the fluorous phase affinity of the free phosphine ligands themselves and is in fact the result of the much higher fluorous phase affinity of the phosphine-containing rhodium species that are present during and after catalysis. Hence it is demonstrated that assembling multiple fluorous ligands in a specific configuration at one metal center can drastically improve the fluorous phase affinity of the resulting complexes.

Introduction

Catalyst recycling and reuse can be of crucial importance in homogeneous catalysis if toxic and/or expensive metal catalysts are involved.[1] To achieve efficient catalyst recovery, while maintaining the high activity and selectivity of nonimmobilized systems, various concepts for catalyst immobilization in the presence of a mobile substrate phase have been developed.[2] In liquid biphasic catalysis the catalyst is immobilized in one of the two phases of a biphasic system consisting of either water and an organic solvent[2a,b] or an ionic liquid and an organic solvent.[2c] Furthermore membrane techniques based on dendrimer- or other macromolecule-attached metal catalysts have been developed.[2d] However, a major disadvantage of these techniques is the reduced activity due to mass-transport limitation as a result of phase boundaries present between reactants and catalysts.

In Fluorous Biphasic Systems (FBS), first applied by Horváth and Vogt[3] as an elegant alternative to aqueous biphasic catalyst separation, this problem is not present because of the unique ability of fluorinated solvents to form mono- or biphasic systems with conventional organic solvents, above and below the consolute temperature, respectively.[4] The major advantage is that the *catalytic reaction* can now be performed above the consolute temperature under truly homogeneous conditions whereas biphasic catalyst *separation* can be accomplished by cooling.

A number of catalytic reactions employing FBS-based separation techniques have been reported: i.e., hydroformylation,[3b−d,5] hydroboration[6] and epoxidation of alkenes,[7] oxidation of hydrocarbons,[8] and cross-coupling and allylic substitution reactions.[9] However, reported turnover frequencies (TOF) and

[†] Debye Institute.
[‡] Bijvoet Center for Biomolecular and Structural Chemistry.
[§] Elf Atochem Vlissingen B.V., currently based at the Debye Institute. E-mail: b.j.deelman@chem.uu.nl. Fax: +31 30 2523615.

(1) Cornils, B.; Herrmann, W. A. In *Applied Homogeneous Catalysis with Organometallic Compounds*; Cornils, B., Herrmann, W. A., Eds.; Weinheim: New York, 1996; Chapter 4.1, pp 1167−1197.

(2) (a) Cornils, B.; Herrmann, W. A. In *Applied Homogeneous Catalysis with Organometallic Compounds*; Cornils, B., Herrmann, W. A., Eds.; Weinheim: New York, 1996; Chapter 3.1, pp 577−600. (b) Chauvin, Y.; Olivier-Bourbigou, H. *CHEMTECH* **1995**, *25*, 26. (c) Chauvin, Y.; Mussmann, L.; Olivier, H. *Angew. Chem., Int. Ed. Engl.* **1995**, *34*, 2698−2700. (d) Knapen, J. W. J.; van der Made, A. W.; de Wilde, J. C.; van Leeuwen, P. W. N. M.; Wijkens, P.; Grove, D. M.; van Koten, G. *Nature* **1994**, *372*, 659−663.

(3) (a) Vogt, M. Ph.D. Thesis, Rheinisch-Westfälische Technische Hochschule, Aachen, Germany, 1991. (b) Horváth, I. T.; Rábai, J. *Science* **1994**, *266*, 72−75. (c) Horváth, I.; Rábai, J. U.S. Patent 5463082, 1995. (d) Horváth, I. *Acc. Chem. Res.* **1998**, *31*, 641−650. (e) Keim, W.; Vogt, M.; Wasserscheid, P.; Driessen-Hölscher, B. *J. Mol. Catal. A: Chem.* **1999**, *139*, 171−175.

(4) De Wolf, E.; Deelman, B.-J.; Van Koten, G. *Chem. Soc. Rev.* **1999**, *28*, 37−41 and references therein.

(5) (a) Kainz, S.; Koch, D.; Baumann, W.; Leitner, W. *Angew. Chem., Int. Ed. Engl.* **1997**, *36*, 1628−1630. (b) Horváth, I. T.; Kiss, G.; Cook, R. A.; Bond, J. E.; Stevens, P. A.; Rábai, J.; Mozeleski, E. J. *J. Am. Chem. Soc.* **1998**, *120*, 3133−3142.

(6) (a) Juliette, J. J. J.; Horváth, I. T.; Gladysz, J. A. *Angew. Chem., Int. Ed. Engl.* **1997**, *36*, 1610−1612. (b) Juliette, J. J. J.; Rutherford, D.; Horváth, I. T.; Gladysz, J. A. *J. Am. Chem. Soc.* **1999**, *121*, 2696−2704.

(7) (a) Pozzi, G.; Banfi, S.; Manfredi, A.; Montanari, F.; Quici, S. *Tetrahedron* **1996**, *52*, 11879−11888. (b) Pozzi, G.; Cinato, F.; Montanari, F.; Quici, S. *Chem. Commun.* **1998**, 877.

(8) (a) Klement, I.; Knochel, P. *Synlett* **1995**, 1113−1115. (b) Vincent, J.-M.; Rabion, A.; Yachandra, V. K.; Fish, R. H. *Angew. Chem., Int. Ed.* **1997**, *36*, 2346−2349. (c) Klement, I.; Lütjens, H.; Knochel, P. *Angew. Chem., Int. Ed. Engl.* **1997**, *36*, 1454−1456. (d) Pozzi, G.; Montanari, F.; Quici, S. *Chem. Commun.* **1997**, 69. (e) Guillevic, M.-A.; Horváth, I. T.; Gladysz, J. A. *Angew. Chem., Int. Ed. Engl.* **1997**, *36*, 1612−1614.

10.1021/ja993562v CCC: $19.00
Published on Web 04/06/2000

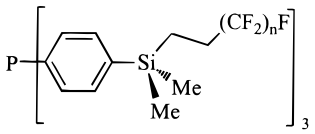

1a: n = 6
1b: n = 8

Figure 1. Fluorous triphenylphosphine derivative with silicon as the branching point and spacer group.

turnover numbers (TON) of fluorous rhodium(I)-catalyzed hydrogenation of terminal and cyclic alkenes which employ fluorous alkylphosphines (TON = 98−120 in 16 h)[10a] or aryl phosphites (TON = 16−1073 in 24 h)[10b] are low and fall far below the activity of Wilkinson's catalyst $RhCl(PPh_3)_3$ (TOF is ca. 150−600 h^{-1} for 1-alkenes).[11,12,16b] One possible explanation could be that the donor properties of the phosphine ligand are influenced in a negative sense by the electron-withdrawing effect of the perfluoro tail. Also in olefin hydroformylation the activity of the $Rh(I)/P[CH_2CH_2(CF_2)_5CF_3]_3$ system was found to be 1 order of magnitude lower than that of $Rh(I)/PPh_3$.[5b] This latter observation is not unexpected because of the demonstrated improvement in the activity of aryl- versus alkylphosphine Rh complexes.[11] Stimulated by these considerations we became interested in using previously developed fluorous triarylphosphines[13] $P[C_6H_4\text{-}p\text{-}SiMe_2(CH_2)_2C_nF_{2n+1}]_3\}_3$ (Figure 1) to obtain analogues of Wilkinson's catalyst[12] and to investigate their potential advantages in the context of homogeneous hydrogenation of 1-alkenes. The weakly electron donating silicon atom, we reasoned, could compensate for the strongly electron withdrawing effect of the fluorotail(s) on the aryl ring preventing a negative influence on the donor properties of the phosphorus atom. Furthermore it has the added advantage that it can serve as a branching point for connecting up to three fluoro tails per aryl ring and provides a means to enhance the fluorous character of the phosphine.[13]

Results and Discussion

Synthesis. Using previously developed fluorous and nonfluorous silyl-substituted triarylphosphines **1**[12,13] (Figure 1), fluorous Rh(I)-complexes **3a**,**b** and the nonfluorous derivative **3c** were synthesized from $[(COD)RhCl]_2$ (COD = 1,5-cyclooctadiene, Scheme 1). Another efficient method to obtain fluorous **3a,b** is the successive substitution of the PPh_3 ligands of $RhCl(PPh_3)_3$ by their fluorous derivatives (Scheme 1).

Scheme 1

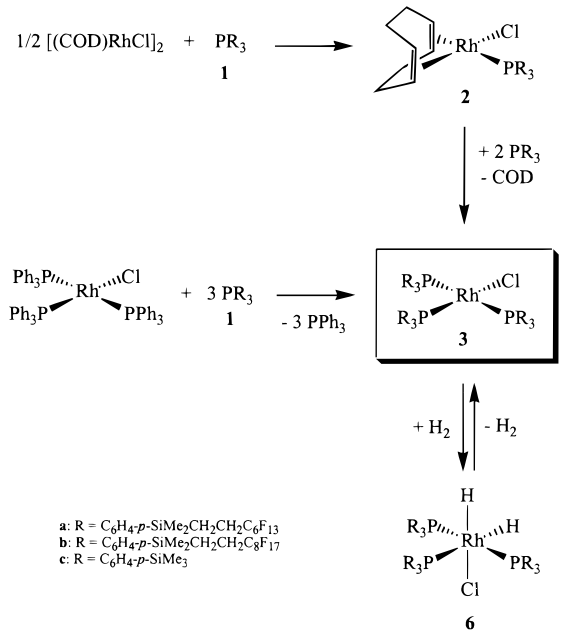

The reaction of $[(COD)RhCl]_2$ with 6 equiv of **1a−c** in benzene was monitored by ^{31}P NMR and found to lead initially to complexes $(COD)RhCl(PR_3)$ (**2a−c**) (δ_P 30.6, d). A mononuclear structure of compounds **2** is proposed on the basis of the $^1J_{Rh,P}$ coupling constant (e.g., 151 Hz for **2a**), which is characteristic for monomeric complexes of this type rather than dimeric alternatives; i.e., a $^1J_{Rh,P}$ coupling constant of 188 Hz was reported for dimeric $[(COE)RhClL]_2$ (COE = cyclooctene) whereas for monomeric (COD)RhClL (L = $P(H)[CH(SiMe_3)_2]_2$) a $^1J_{Rh,P}$ of 151 Hz was found.[14a] Complexes **2** were obtained as dark red viscous oils (**2a**,**b**) contaminated with **1** and **3** or as yellow solid (**2c**). Complex **2c**, being less soluble in *n*-pentane than **3c**, was easily purified by recrystallization. If allowed to react further for 12−15 h complexes **3a**,**b** were obtained as dark red viscous oils, which separated from the aromatic solvent and contained 10 to 30% of uncoordinated phosphine. However, decantation of the upper organic phase and washing of the remaining oil with toluene or benzene yielded analytically pure complexes **3a** and **3b** in reasonable to high yields (44 and 87%, respectively). These novel complexes were characterized by ^1H, ^{31}P, and ^{13}C NMR (**2a**) spectroscopy.

From the chemical shift and the $J_{Rh,P}$ and $J_{P,P}$ values for **3** in comparison with $RhCl(PPh_3)_3$ and $RhCl[P(C_6H_4\text{-}p\text{-}Me)_3]_3$ (Table 1) it is clear that similar square-planar structures are retained in solution. In particular from the very similar $J_{Rh,P}$ coupling constants it can be concluded that the character of the Rh−P bond is not influenced significantly by the presence of the perfluoro tails, thereby reflecting comparable electronic surroundings for the rhodium centers in **3** and nonfluorous derivatives **3c**, $RhCl(PPh_3)_3$, and $RhCl[P(C_6H_4\text{-}p\text{-}Me)_3]_3$. Hence similar catalytic activity would be expected. Furthermore, the formation of complexes **3** via substitution of the COD ligand in **2** indicates that phosphines **1** belong to the group of sterically less demanding phosphines such as PPh_3, $PPhMe_2$, and $P(^nBu)_3$ since more bulky phosphines are known to prohibit the formation of compounds with cis-positioned ligands.[14]

(9) (a) Betzemeier, B.; Knochel, P. *Angew. Chem., Int. Ed. Engl.* **1997**, *36*, 2623−2624. (b) Caroll, M. A.; Holmes, A. B. *Chem. Commun.* **1998**, 1395−1396. (c) Kling, R.; Sinou, D.; Pozzi, G.; Chopin, A.; Quignard, F.; Busch, S.; Kainz, S.; Koch, D.; Leitner, W. *Tetrahedron Lett.* **1998**, *39*, 9439−9442.

(10) (a) Rutherford, D.; Juliette, J. J. J.; Rocaboy, C.; Horváth, I. T.; Gladysz, J. A. *Catal. Today* **1998**, *42*, 381−388. (b) Haar, C. M.; Huang, J.; Nolan, S. P.; Petersen, J. L. *Organometallics* **1998**, *17*, 5018−5024.

(11) (a) Chaloner, P. A.; Esteruelas, M. A.; Joó, F.; Oro, L. A. *Homogeneous Hydrogenation*; Kluwer: Boston, 1994; pp 8−9. (b) Montelatici, A.; van der Ent, A.; Osborn, J. A.; Wilkinson, G. *J. Chem. Soc. (A)* **1968**, 1054−1058. (c) Jardine, F. H. In *Prog. Inorg. Chem.***1981**, *28*, 117−131.

(12) (a) Richter, B.; Deelman, B.-J.; van Koten, G. European Patent Appl. 98203308.6. (b) Richter, B.; Deelman, B.-J.; van Koten, G. *J. Mol. Catal. (A), Chem.* **1999**, *145*, 317. (c) Deelman, B.-J.; Richter, B.; Van Koten, G. *CERC3 Young Chemists Workshop "Homogeneous Catalysis"*; University of Rostock, April 21−24, 1999; Book of abstracts. (d) Deelman, B.-J.; Richter, B.; Van Koten, G. *218th American Chemical Society National Meeting*; New Orleans, August 22−26, 1999, New Orleans, Louisiana; American Chemical Society: Washington, DC, 1999; Book of abstracts.

(13) Richter, B.; de Wolf, E.; Deelman, B.-J.; van Koten, G. *J. Org. Chem.* Accepted for publication.

(14) (a) Murray, B. D.; Hope, H.; Hvoslef, J.; Power, P. P. *Organometallics* **1984**, *3*, 657−663. (b) Denise, B.; Pannetier, G. *J. Organomet. Chem.* **1978**, *148*, 155.

(15) (a) Tolman, C. A.; Meakin, P. Z.; Lindner, D. L.; Jesson, J. P. *J. Am. Chem. Soc.* **1974**, *96*, 2762−2774. (b) Halpern, J.; Okamoto, T.; Zakhariev A. *J. Mol. Catal.* **1976**, *2*, 65−69.

(16) (a) Young, J. F.; Osborn, J. A.; Jardine, F. H.; Wilkinson, G. *Chem. Commun.* **1965**, 131−132. (b) Osborne, J. A.; Jardine, F. H.; Young, J. F.; Wilkinson, G. *J. Chem. Soc. (A)* **1966**, 1711−1732. (c) Osborn, J. A.; Wilkinson, G. *Inorg. Synth.* **1967**, *10*, 67−71. (d) Jardine, F. H.; Osborn, J. A.; Wilkinson, G. *J. Chem. Soc. (A)* **1967**, 1574−1578.

Table 1. ^{31}P NMR Data and Assignment for the Fluorous Wilkinson-Type and Related Complexes[a]

complex	*trans*-P−Rh-X (X = Cl, O, H)			trans-P−Rh−P		
	δ_P (multiplicity)	$^1J_{Rh,P}$ (Hz)	$^2J_{P,P}$ (Hz)	δ_P (multiplicity)	$^1J_{Rh,P}$ (Hz)	$^2J_{P,P}$ (Hz)
(COD)RhCl[P{C_6H_4-*p*-$SiMe_2Rf_6$}$_3$] (**2a**)[b]	30.6 (d)	151				
(COD)RhCl[P{C_6H_4-*p*-$SiMe_2Rf_8$}$_3$] (**2b**)[b]	30.7 (d)	154				
(COD)RhCl[P{C_6H_4-*p*-$SiMe_3$}$_3$] (**2c**)[b]	30.7 (d)	151				
$RhCl(PPh_3)_3$[b]	48.1 (dt)	190	37.9	31.2 (dd)	145	37.8
$RhCl[P(C_6H_4$-*p*-$SiMe_2$-$Rf_6)_3]_3$ (**3a**)[c]	48.0 (dt)	190	37.8	31.4 (dd)	143	37.6
$RhCl[P(C_6H_4$-*p*-$SiMe_2$-$Rf_8)_3]_3$ (**3b**)[d]	48.0 (dt)	192	37.8	31.4 (dd)	145	37.4
$RhCl[P(C_6H_4$-*p*-$SiMe_3)_3]_3$ (**3c**)[b]	47.4 (dt)	192	37.6	31.0 (dd)	143	37.5
$RhCl[P(C_6H_4$-*p*-$Me)_3]_3$[e]	46.2 (dt)	189	38	30.2 (dd)	143	38
$RhCl[P(C_6H_4$-*m*-$Rf_6)_3]_3$[f]	51.1 (dt)	188	38	36.2 (dd)	142	38
$[RhCl(PPh_3)_2]_2$[b]	52.8 (d)	195				
$[RhCl\{P(C_6H_4$-*p*-$SiMe_2$-$Rf_6)_3\}_2]_2$ (**4a**)[c]	50.0 (d)	198				
$[RhCl\{P(C_6H_4$-*p*-$SiMe_2$-$Rf_8)_3\}_2]_2$ (**4b**)[b]	51.4 (d)	196				
$[RhCl\{P(C_6H_4$-*p*-$SiMe_3)_3\}_2]_2$ (**4c**)[b]	51.8 (d)	195				
$[RhCl\{P(C_6H_4$-*p*-$Me)_3\}_2]_2$[e]	49.5 (d)	196				
$RhCl(O_2)[P(C_6H_4$-*m*-$SO_3Na)_3]_3$[i]	28.2 (dt)	151	24	17.5 (dd)	98	24
$RhCl(O_2)[P(C_6H_4$-*p*-$SiMe_2$-$Rf_6)_3]_3$ (**5a**)[b]	26.3 (dt)	151	25.8	12.0 (dd)	99.6	25.5
$RhCl(O_2)[P(C_6H_4$-*p*-$SiMe_2$-$Rf_8)_3]_3$ (**5b**)[b]	28.0 (dt)	152	25.5	13.7 (dd)	99.6	25.5
$RhCl(O_2)[P(C_6H_4$-*p*-$SiMe_3)_3]_3$ (**5c**)[b]	28.1 (dt)	152	25.5	14.2 (dd)	99.7	25.5
cis-$RhCl(H)_2(PPh_3)_3$[j]	20.7 (dt)	90	17.5	40.3 (dd)	114	17.5
cis-$RhCl(H)_2[P(C_6H_4$-*p*-$SiMe_2$-$Rf_6)_3]_3$ (**6a**)[b]	19.9 (dt)	89.6	*g*	39.9 (dd)	116	19.0
cis-$RhCl(H)_2[P(C_6H_4$-*p*-$SiMe_2$-$Rf_8)_3]_3$ (**6b**)[h]	19.7 (dt)	88.4	18.3	41.1 (dd)	114	18.2
cis-$RhCl(H)_2[P(C_6H_4$-*p*-$SiMe_3)_3]_3$ (**6c**)[b]	19.3 (dt)	91.5	*g*	39.9 (dd)	115	14.7

[a] $Rf_6 = CH_2CH_2(CF_2)_5CF_3$; $Rf_8 = CH_2CH_2(CF_2)_7CF_3$. [b] C_6D_6. [c] FC-72/C_6D_6, 1:1 (v/v). [d] $CF_3C_6H_5/C_6D_6$, 1:1 (v/v). [e] $C_6H_5CH_3$, see ref 15. [f] THF-d_8, see ref 5a. [g] not resolved. [h] *n*-C_6D_{14}/FC-72 1:1 (v/v). [i] H_2O, see ref 17c. [j] At −25 °C, CH_2Cl_2, see ref 15a.

Scheme 2

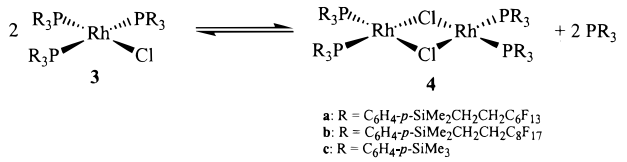

An attempt to convert a mixture of **1a**, **2a**, and **3a** completely to **3a** by hydrogenation of the COD ligand under a dihydrogen atmosphere (1 bar) failed and led to the formation of a cis dihydride species **6a** whereas **2a** remained unchanged. The pale yellow cis dihydride complexes **6** can be reconverted into square-planar **3** by dihydrogen elimination under reduced pressure or by the addition of an excess of 1-hexene. ^{1}H and ^{31}P NMR data indicate that complexes **6** under a dihydrogen atmosphere exhibit octahedral structures with one hydride trans to phosphorus (**6c**: doublet, $\delta_H = -9.1$, $^2J_{H,P} = 141$ Hz) and the other located trans to the chloride ligand (**6c**: singlet, $\delta_H = -16.5$). Related compounds are well-known for PPh_3[15] and also for fluorous alkylphosphine $P(CH_2CH_2C_6F_{13})_3$.[10a]

The substitution of PPh_3 in $RhCl(PPh_3)_3$ by its fluorous and nonfluorous phosphines **1** was demonstrated for **3b** and **3c**. In the case of **3b** the complex precipitated as a red oil from benzene. In contrast, treatment of $RhCl(PPh_3)_3$ with **1c** (3 equiv and excess) led to the formation of a complicated mixture of several mixed phosphine complexes. These results indicate that there is a significant shift of the equilibrium for **1b** toward complete PPh_3 substitution, which is most probably driven by the decreased solubility of the fluorous complex **3b** in benzene.

The equilibrium of the square-planar complex $RhCl(PPh_3)_3$ with the dimeric species $[RhCl(PPh_3)_2]_2$ and free ligand in solution is well-known (Scheme 2).[11b,16] In the case of $RhCl(PPh_3)_3$ itself, a dimer-to-monomer ratio amounting to 0.2 was found in $CF_3C_6H_5/C_6D_6$ as solvent (1:1 (v/v), 25 °C). Complexes **3a** and **3b** show a similar behavior. However, in the presence of an excess of 10 mol % of free ligand (relative to **3a**,**b**) the dimer-to-monomer ratio was found to be <0.01.

The oxygen sensitivity of $RhCl(PPh_3)_3$ and its derivatives has long been noted[17] and was also observed for complexes **3a**−**c**.

Scheme 3

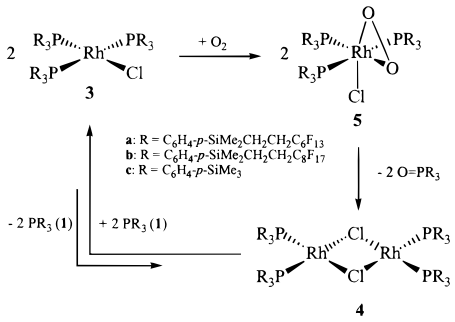

The presence of oxygen causes the formation of the η^2-O_2-complexes **5a**−**c** (^{31}P NMR, Table 1), which decompose over a period of days affording dimeric complexes **4** and fluorous triarylphosphine oxide ($O{=}PR_3$ in Scheme 3) which is in line with earlier observations for $RhCl(PPh_3)_3O_2$.[17e] If excess of free phosphine **1** is added either initially or after initial reaction with oxygen (2 equiv per Rh), rhodium-catalyzed oxidation of phosphine takes place[17e] with compounds **1**, **3**, and $O{=}PR_3$ as the sole species present in the final product mixture (Scheme 3). The ^{31}P NMR spectroscopic data of oxo complexes **5** are in close agreement with data reported for $RhCl(O_2)[P(C_6H_4$-*m*-$SO_3Na)_3]$ (Table 1).[17c]

The results of an X-ray structural analysis of **4c** indicate that its molecular structure (Figure 2) is analogous to the dimeric structure displayed by $[Rh(\mu$-$Cl)(PPh_3)_2]_2$.[18a] The Rh−Cl and Rh−P bond lengths in **4c** (2.408(5) Å (Rh−Cl), 2.394(5) Å (Rh−Cl(a)), 2.220(5) Å (Rh−P(1)), and 2.211(5) Å (Rh−P(2)) are within experimental error comparable to the corresponding distances in $[RhCl(PPh_3)_2]_2$ (2.394(2) Å (Rh−Cl), 2.424(2) Å (Rh−Cl′), 2.200(2) Å (Rh−P(1)) and 2.213(2) Å (Rh−P(2)), respectively. However, in contrast to $[RhCl(PPh_3)_2]_2$, **4c** has a

(17) (a) Baird, M. C.; Lawson, D. N.; Mague, J. T.; Osborn, J. A.; Wilkinson, G. *Chem. Commun*. **1966**, 129. (b) Bennett, M. J.; Donaldson, P. B. *Inorg. Chem.* **1977**, *16*, 1581−1585. (c) Larpent, C.; Dabard, R.; Patin, H. *New J. Chem*. **1988**, *12*, 907. (d) Suzuki, H.; Matsuura, S.; Moro-Oka, Y.; Ikawa, T. *J. Organomet. Chem.* **1985**, *286*, 247−258. (e) Atlay, M. T.; Carlton, L.; Read, G. *J. Mol. Catal.* **1983**, *19*, 57.

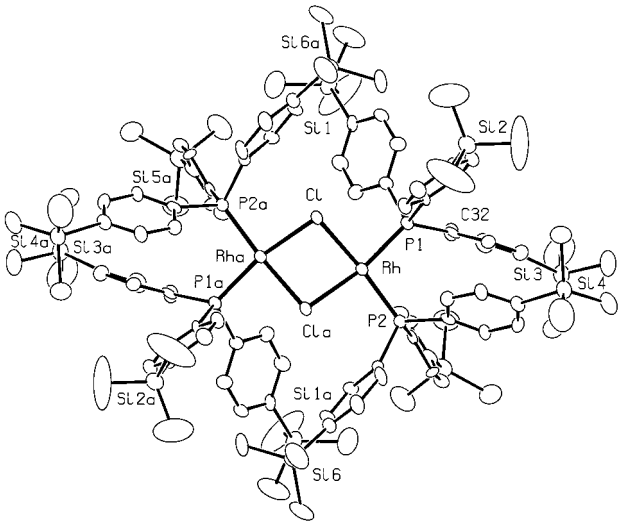

Figure 2. Displacement ellipsoid illustration of **4c** at the 30% probability level. Hydrogen atoms and disordered solvent were omitted. Selected bonding distances (Å) and angles (deg): Rh···Rh(A) = 3.450(5), Rh−Cl = 2.408(5), Rh−Cl(a) = 2.394(5), Rh−P(1) = 2.220-(5), Rh−P(2) = 2.211(5), P(1)−C(11) = 1.820(14), P(1)−C(21) = 1.837(12), P(1)−C(31) = 1.848(11), P(2)−C(41) = 1.851(11), P(2)−C(51) = 1.817(12), P(2)−C(61) = 1.823(14), Cl−Rh−P(1) = 87.97(14), Cl−Rh−P(2) = 172.10(14), Cl−Rh−Cl(a) = 80.78(14), P(1)−Rh−P(2) = 97.83(15), P(1)−Rh−Cl(a) = 168.63(15), Rh−Cl−Rh(a) = 91.86(15), C(11)−P(1)−C(21) = 104.7(6), C(11)−P(1)−C(31) = 100.3(6), C(21)−P(1)−C(31) = 103.0(5), C(41)−P(2)−C(51) = 105.4(5), C(41)−P(2)−C(61) = 102.4(5), C(51)−P(2)−C(61) = 101.5(6).

folded Rh(μ-Cl)$_2$Rh moiety (fold angle (λ) = 141.3(2)°), which is the largest value for nonplanar structures of this type (λ is usually <134°).[18] As a consequence the intramolecular Rh−Rh distance of 3.449(5) Å is around 0.2 to 0.4 Å longer compared to other folded structures.[18] Recent discussions propose steric (cone angle and interligand repulsion) rather than electronic features of the phosphine as the origin of a more or less folded moiety.[18c] Extended Hückel calculations using [RhCl(PH$_3$)$_2$]$_2$ and [RhCl(dphm)]$_2$ (dphm = H$_2$PCH$_2$PH$_2$) as model compounds resulted in planar structures being the most stable ones but also revealed an energy cost of only 10 kJ mol^{-1} to fold these structures to λ = 140°. Hence, packing effects and/or subtle intramolecular steric interactions will most probably be sufficient to determine the actual folding angle in the solid state.

Catalytic Hydrogenation. Rhodium complexes **3a**,**b** obtained from [(COD)RhCl]$_2$ and fluorous phosphines **1a**,**b** were found to be active catalysts for hydrogenation of 1-alkenes under single-phase fluorous conditions at 80 °C (Table 2). The hydrogenation products were readily isolated from the catalyst layer by cooling of the reaction mixture to 0 °C followed by phase separation of the resulting biphasic system. In this way hydrogenation of 1-octene afforded *n*-octane in >95% yield (GC, GC-MS). Less than 4.3% internal olefins resulting from isomerization were present. In the case of **3b** we were able to recycle the fluorous catalyst layer multiple times while still maintaining high turnover numbers and high conversions per cycle (Table 2 and Figure 3).

(18) (a) Curtis, D. M.; Butler, W. M.; Greene, J. *Inorg. Chem.* **1978**, *17*, 2928−2931. (b) Kubas, G. J.; Ryan, R. R. *Cryst. Struct. Commun.* **1977**, *6*, 295−300. (c) Wang, K.; Goldman, M. E.; Emge, T. J.; Goldman, A. S. *J. Organomet. Chem.* **1996**, *518*, 55−68. (d) Hofmann, P.; Meier, C.; Hiller, W.; Heckel, M.; Riede, J.; Schmidt, M. U. *J. Organomet. Chem.* **1995**, *490*, 51−70.

Table 2. Catalytic Hydrogenation[a] of 1-Octene Using **3a,b** as Pre-catalysts

complex	cycle	conv (%)	$t_{1/2}$ (min)	TOF$_{50\%}$ (h^{-1})	TON (cumulative)	leaching (%)[b] Rh	P
3a[c]	1	95	56	298	531	0.27	8.10
3b[d]	1	92	69	177	337	0.11	2.34
	2	96	58	212	688	0.05	2.06
	3	99	47	261	1048	0.10	3.24
	4	92	43	277	1383	0.11	3.20
	5	99.8	40	304	1747	0.18	3.52
	6	96.8	30	397	2100	0.08	2.15
	7	94	24	507	2444	0.05	2.43
	8	99.7	20	617	2808	0.33[e]	4.70[e]
	9[f]	85	75	142	3117	0.08	3.41

[a] Conditions: solvent = *c*-CF$_3$C$_6$F$_{11}$, T = 80 °C, p(H$_2$) = 1 bar. [b] At T = 0 °C, estimated error of ICP-AAS analysis ±0.013%. [c] Containing 10% of **1a**, [1-octene]/[Rh] = 521, [Rh]$_0$ = 0.0060 mol/L. [d] [1-octene]/[Rh] = 365, [Rh] = 0.0087 mol/L in the initial cycle. [e] High value due to experimental error during phase separation. [f] Fresh *c*-CF$_3$C$_6$F$_{11}$ was added as compensation for losses of fluorous solvent to reestablish the starting conditions (see text).

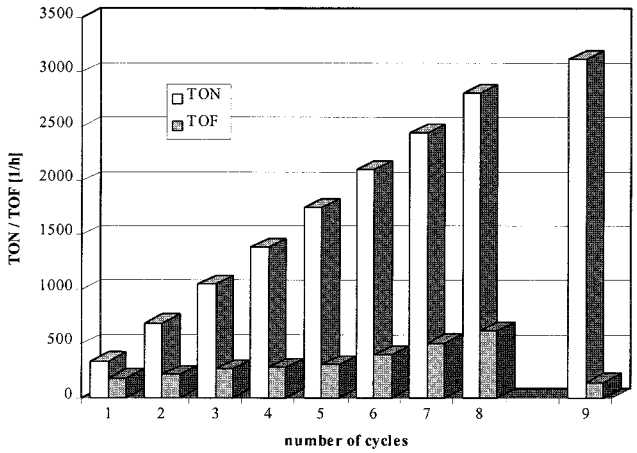

Figure 3. Plot of the turnover number (TON) and turnover frequency (TOF) for nine cycles. Conditions: catalyst = RhCl[P(C$_6$H$_4$-*p*-SiMe$_2$-(CH$_2$)$_2$(CF$_2$)$_7$CF$_3$)$_3$]$_3$; solvent = CF$_3$C$_6$F$_{11}$; T = 80 °C; p(H$_2$) = 1 bar; [1-octene]/[Rh] = 365; [Rh]$_0$ = 0.0087 mol/L. Fresh *c*-CF$_3$C$_6$F$_{11}$ was added in the 9th cycle as compensation for losses of fluorous solvent to reestablish the starting conditions (see text).

It was found for **3b** that the activity increased with the number of cycles (up to TOF ~ 600 h^{-1} in the 8th cycle). This is most probably caused by the combined effects of a non-zero-order rate dependence in rhodium and the (observed) loss of fluorous solvent due to evaporation during phase separation under H$_2$ -flow and nonzero miscibility of *c*-C$_6$F$_{11}$CF$_3$ in the product layer even at 0 °C (ca. 5 vol %). Consequently, an average loss of fluorous solvent of ca. 12% per cycle (ca. 0.25 mL) took place. However, restoring the amount of *c*-C$_6$F$_{11}$CF$_3$ in the 9th cycle to its initial volume showed that the catalyst activity had dropped only by 19% (entry 9, Table 2).

As anticipated from the limited drop in activity upon recycling of the catalyst layer resulting from **3b**, rhodium leaching into the organic phase (as determined by ICP-AAS) was indeed low. On average 0.12% of Rh per cycle was lost corresponding to a rhodium concentration of 3 ppm (by weight) in the product phase. Over 9 cycles only 1% of rhodium was lost despite the rather simple phase separation method used. Not surprisingly, leaching was higher for the pre-catalyst with a lower fluorine content, e.g., for **3a**, 0.3% (6 ppm) of rhodium was present in the organic phase after phase separation.

The amount of leached rhodium enabled us to calculate the average partition coefficients (P) of the rhodium species present

Table 3. Average Partition Coefficients (P)[a] of Rhodium Species Present in the Fluorous Biphasic Product Mixture Resulting from Hydrogenation of 1-Octene

pre-catalyst	F-content of phosphine (wt %)	P	
		$T = 25$ °C	$T = 0$ °C
3a	48.7	76	293
3b	53.2	n.d.	887

[a] Calculated from the amount of Rh found in the organic product phase of the first cycle by ICP-AAS analysis.

during phase separation (Table 3). The values found clearly demonstrate a significant positive effect of longer fluorochains and lower temperature. The partitioning of rhodium found for **3b** at 0 °C is higher than that reported for $RhCl[P(CH_2)_2(CF_2)_nCF_3)_3]_3$ (696 and 811 for $n = 5$ and 7, respectively, in c-$C_6F_{11}CF_3$/toluene at 27 °C).[6b] Although a direct comparison is not possible because of the different solvent system used, this result is still surprisingly good for arylphosphine rhodium complexes taking into account the significant lower partition coefficients of the fluorous arylphosphines (**1a**, $P = 0.26$; **1b**, $P = 2.2$, in c-$C_6F_{11}CF_3$/toluene at 0 °C)[12] as compared to the fluorous alkylphosphines $P[(CH_2)_2(CF_2)_nCF_3)_3]_3$ ($n = 5$, $P = 82$ and $n = 7$, $P = 332$ in c-$C_6F_{11}CF_3$/toluene at 27 °C).[6a] This result emphasizes that the fluorophase preference of the rhodium complexes cannot solely be deduced from the partition coefficient of the phosphine ligand itself, although an increase of fluorphase affinity of the phosphine does correspond to a higher fluorphase affinity of the derived Rh complex. This latter observation also becomes apparent if the improvement in fluorphase partitioning of **1b** relative to **1a** is compared with the higher fluorphase partition coefficient of **3b** relative to **3a**. Clearly the relative orientation of the phosphine ligands in the derived rhodium complexes is important. A fluorophilic van der Waals surface, made up of a relatively high proportion of CF_2 and CF_3 units that shield the fluorophobic metal environment of the catalyst, may well be a prerequisite for high fluorphase affinity and hence good recycling efficiency in fluorous biphasic separation.

It should be noted that efficient retention of uncoordinated fluorous phosphine in the fluorphase is as important for recycling the intact catalyst system as is retention of rhodium. In fact, significant amounts of fluorous phosphine were present in the alkane product phases (**3a** (**3b**): 130 (64) ppm, corresponding to 8.1 (3.0)% of total phosphorus present in the precatalyst) indicating that leaching of fluorous ligand is more significant than that of rhodium itself and to a large extent responsible for the low recycling efficiency of the **3a**-derived catalyst solution. A monomer−dimer equilibrium involving dissociation of phosphine as in Scheme 2 or more likely one involving dissociation of phosphine from dihydrides **6** which are the predominant species present under dihydrogen atmosphere[16] may well be responsible for this behavior (eq 1).

$$\underset{\mathbf{6}}{RhH_2Cl(PR_3)_3} \rightleftharpoons RhH_2Cl(PR_3)_2 + PR_3 \quad (1)$$

R = -C_6H_4-*p*-$SiMe_2CH_2CH_2$ C_6F_{13} (**a**)
R = -C_6H_4-*p*-$SiMe_2CH_2CH_2$ C_8F_{17} (**b**)

To allow comparison of the activities of fluorous derivatives **3a** and **3b** with those of nonfluorous **3c** and conventional Wilkinson catalyst $RhCl(PPh_3)_3$, 1-octene hydrogenation experiments under single-phase conditions in the hybrid solvent α,α,α-trifluorotoluene at atmospheric dihydrogen pressures were carried out. The results obtained with the different pre-catalysts are listed in Table 4. Highest rates of dihydrogen uptake (14.2 mol·L^{-1}·h^{-1}) were measured for **3c** at relatively high rhodium and olefin concentrations (entry 2, Table 4). Under these conditions a zero-order dependence in [1-octene] was found up to ca. 80% conversion resulting in a linear conversion versus time plot. In all other experiments ([Rh] = 4.0−8.0 mM, $[1\text{-octene}]_0 = 1.46$ M) rates of dihydrogen uptake were lower (<11 mol·L^{-1}·h^{-1}) and conversion versus time plots corresponded to a rate law $-d[1\text{-octene}]/dt = k_{obs}[1\text{-octene}]$ for >98% conversion, which allows the catalyst activity to be evaluated in terms of the observed first-order rate constant k_{obs}. Because the rates of dihydrogen uptake for these experiments were well below the maximum value obtained in entry 2, diffusion limitation of dihydrogen can be excluded in these cases. In addition to k_{obs}, turnover frequencies (TOF in mol·mol^{-1}·h^{-1}) were derived from the tangent of a 4th order polynomal fit to conversion versus time plots at 25% conversion and served as a measure of catalyst activity independent of any assumed kinetic relationship with substrate.

From Table 4 it is clear that **3c** displays by far the highest activity being >1.5 times more active than Wilkinson's catalyst. This result clearly shows the beneficial influence of the *p*-silyl substitution on catalytic activity. However, the most important observation is the fact that **3a** (entry 3) is comparable in activity to $RhCl(PPh_3)_3$ (entry 4) despite its fluoro-tail functionalization and the presence of small quantities of free phosphine (<10%), which is known to inhibit catalytic activity.[11b,c] The somewhat lower activity of **3b** (entry 5) suggests a small negative electronic influence on catalytic activity caused by the longer fluorotail. However, solvation effects cannot be excluded either. The overall activities of **3a** and **3b** in perfluoromethylcyclohexane and solvent α,α,α-trifluorotoluene also compare favorably with turnover frequencies for 1-alkene hydrogenation by the Wilkinson catalyst in conventional solvents (TOF = 150−600 h^{-1} for hydrogenation of 1-heptene in benzene).[16b]

The overall first-order kinetics observed are noteworthy. More complicated relationships between substrate concentration and rate of hydrogenation are found in the literature (e.g. $1/\text{rate} = C(1/[\text{olefin}]) + C'$ with C and C' being constants),[16b] which is due to parasitic formation of inactive olefin complexes $RhClP_2$(olefin) (P = phosphine), especially at higher olefin concentrations. Our data appear to be in line with the conventional hydrogenation mechanism proposed for Wilkinson's catalyst, involving rate-limiting elimination of alkane from a dihydrido olefin species which itself is formed in a rapid preequilibrium with dihydride species and olefin[15b] but without kinetically important formation of $RhClP_2$(olefin) complexes. Although we did not study this further, the insignificance of such species under our conditions might well be the result of the different solvent properties of the partially fluorinated solvent α,α,α-trifluorotoluene.

Conclusions

The catalytic results presented above indicate that as far as hydrogenation of 1-alkenes is concerned we have indeed designed and prepared a fluorous alternative to Wilkinson's catalyst with the added advantage of facile catalyst separation and recycling. Recycling efficiencies are >98% (as defined by phosphine leaching and activity) for the catalysts with the longer fluortails (**3b**). This recycling efficiency is much better than expected on the basis of the fluorous phase affinity of the free phosphine ligands alone and is in fact the result of the much higher fluorous phase affinity of the phosphine-containing rhodium species that are present during and after catalysis. It is proposed that this unprecedented effect is a reflection of the

Table 4. Comparison of the Different Pre-catalysts $RhCl[P(C_6H_4\text{-}p\text{-}R)_3]_3$ in the Hydrogenation of 1-Octene[a]

entry	R	[Rh] (mM)	[1-octene] (M)	conversion (%)	TON[b]	k_{obs}[c] (h^{-1})	$TOF_{(25\%)}$[d] (h^{-1})
1	Me_3Si (**3c**)	4.0	1.46	92	336	7.5(2)	1610
2	Me_3Si (**3c**)	8.0	2.92	99	361	*e*	1910
3	$Rf_6(CH_2)_2SiMe_2$ (**3a**)[f]	4.0	1.46	99	363	4.2(1)	1110
4	H	4.0	1.46	98	358	4.0(1)	960
5	$Rf_8(CH_2)_2SiMe_2$ (**3b**)[g]	4.0	1.46	99	355	3.2(1)	870

[a] Conditions: $T = 80$ °C, $p(H_2) = 1$ bar, solvent = α,α,α-trifluorotoluene, stirring speed = 900 rpm. [b] TON = turnover number (mole of olefin/mole of Rh). [c] Obtained by fitting the data to $X_t = [1 - \exp(-k_{obs}t)]$ (X_t = conversion). [d] TOF = turnover frequency (mole of olefin/mole of Rh/hour) at 25% conversion. [e] Zero order in olefin up to 80% conversion, $k_{obs} = 14.2(1)$ mol·L^{-1}·h^{-1}. [f] Rf_6: $-(CF_2)_5CF_3$. [g] Rf_8: $-(CF_2)_7CF_3$.

particular spatial orientation of multiple fluorous ligands assembled on one metal center resulting in a highly fluorous van der Waals surface. Catalytic activities as measured in $C_6H_5CF_3$ are remarkably close to Wilkinson's catalyst stressing the successful application of the $-SiCH_2CH_2-$ spacer in fluorotail functionalization of homogeneous catalysts. Since is was found that catalyst recovery critically depends on the amount of fluorous character of the ligand, we now seek to prepare ligands that give rise to increased fluorous van der Waals surfaces and to employ them in catalysis.[13]

Experimental Section

General Comments and Materials. All reactions and workups were conducted under nitrogen atmosphere unless noted otherwise. Solvents were employed as follows: *c*-$C_6F_{11}CF_3$, $CF_3C_6H_5$ (Acros, Alfa) degassed and stored over molecular sieves; C_6F_6 (Acros), C_6D_6, $CDCl_3$, *n*-C_6D_{14} (Cambridge Isotope Laboratories, Aldrich) degassed and stored over molecular sieves; and 1-octene degassed and distilled over sodium sand. Hydrogen gas (Hoekloos, 5.0) was used as received. Elemental analyses and ICP-AAS measurements were carried out by H. Kolbe, Microanalytisches Laboratorium, Mühlheim an der Ruhr. NMR spectra were obtained from Varian INOVA 300 and MERCURY 200 spectrometers. ^1H, ^{13}C, ^{29}Si NMR spectra are referenced relative to TMS, ^{31}P NMR relative to 85% H_3PO_4, and ^{19}F NMR relative to $CFCl_3$ (external standard). The ^{19}F-decoupler frequency in $^{13}C\{^{19}F\}$NMR experiments was set to δ −121 to decouple from either the ^{19}F-nuclei or the CF_2-moieties. GC analyses were performed on UNICAM PU610 apparatus with a 30 m J&W Scientific AT-SILAR capillary column and a flame ionization detector. Product yields were determined by peak area analysis using *n*-decane as the internal standard. $[(COD)RhCl]_2$ and $RhCl(PPh_3)_3$ were prepared as described in the literature.[19]

Preparation of (COD)RhClP[C_6H_4-*p*-$SiMe_2(CH_2)_2(CF_2)_5CF_3$]$_3$ (2a) and RhCl[P{C_6H_4-*p*-$SiMe_2(CH_2)_2(CF_2)_5CF_3$}$_3$]$_3$ (3a). 1a (3.210 g, 2.176 mmol) dissolved in 20 mL of *n*-hexane and 5 mL of toluene was treated with 0.179 g (0.363 mmol) of $[(COD)RhCl]_2$ at 25 °C. After the solution was stirred for 15 h the volume was reduced by two-thirds and toluene was added (20 mL). Stirring was continued for 15 min affording a biphasic system. The upper phase was carefully decanted and evaporated to dryness affording a red viscous oil, which consisted of **1a**, **2a**, and **3a** (3.5:1:1.5 molar ratio). The fluorous phase consisting of a dark red oil was washed two times with toluene (10 mL) and predried in vacuo (0.1 bar). Further drying in high vacuum (10^{-6} bar) for 12 h afforded 1.50 g of a highly viscous dark red oil containing **3a** (0.318 mmol, 43.8% based on Rh) and 0.1 equiv of **1a**. **2a**: ^1H NMR (200 MHz, C_6D_6): δ 7.92 (m, 6 H, *o*-H, Si-C_6H_4), 7.22 (m, 6 H, *m*-H, Si-C_6H_4), 5.94 (s, 2 H, COD), 3.28 (s, 2 H, COD), 2.18 (m, 2 H, COD), 1.67 (dm, 4 H, COD), 1.85 (m, 6 H, CH_2CF_2), 0.78 (m, 6 H, CH_2Si), −0.02 (s, 36 H, Me). $^{13}C\{^1H\}$ -NMR (75.5 MHz, C_6D_6): δ 140.5 (s, *ipso*-C, Si-C_6H_4), 135.2 (d, $J_{P,C} = 10$ Hz, C_6H_4), 133.7 (d, $J_{P,C} = 10$ Hz, C_6H_4), 119.3 (tt, $^1J_{C,F} = 253$ Hz, $^2J_{C,F} = 32.9$ Hz, α-CF_2), 118.1 (qt, $^1J_{C,F} = 290$ Hz, $^2J_{C,F} = 32.9$ Hz, CF_3), 112.2 (tquin, $^1J_{C,F} = 268$ Hz, $^2J_{C,F} = 31.4$ Hz, *β*-CF_2), 112.1 (tquin, $^1J_{C,F} = 271$ Hz, $^2J_{C,F} = 31.4$ Hz, *γ*-CF_2), 111.3 (tquin, $^1J_{C,F} = 273$ Hz, $^2J_{C,F} = 31.7$ Hz, *δ*-CF_2), 109.4 (tqt, $^1J_{C,F} = 260$ Hz, $^2J_{C,F} = 30.5$ Hz, *ϵ*-CF_2), 106.3 (*δ*-C, COD), 71.0 (d, $^1J_{C,Rh} = 13.1$ Hz, α-C, COD), 33.7 (*β*-C, COD), 29.5 (*γ*-C, COD), 26.5 (t, $^2J_{C,F} = 23.0$ Hz, CH_2CF_2), 5.51 (s, $^1J_{C,Si} = 50.2$ Hz, CH_2Si), −3.69 (s, $^1J_{C,Si} = 54.8$ Hz, Me). **3a**: $C_{144}H_{126}F_{117}ClSi_9P_3Rh$: calcd C 37.9, H 2.78, F 48.71, Si 5.54, P 2.04; found C 37.76, H 2.85, F 48.48, Si 5.61, P 2.11. ^1H NMR (300 MHz, FC-72/C_6D_6, 1:1 (v/v)): δ 7.61 (m, 18 H, *o*-H, Si-C_6H_4), 6.97 (m, 18 H, *m*-H, Si-C_6H_4), 1.87 (m, 18 H, CH_2CF_2), 0.80 (m, 18 H, CH_2Si), 0.04 (m, 54 H, Me).

Preparation of (COD)RhCl[P{C_6H_4-*p*-$SiMe_2(CH_2)_2(CF_2)_7CF_3$)}$_3$] (2b) and RhCl[P{$C_6H_4$-*p*-$SiMe_2(CH_2)_2(CF_2)_7CF_3$}$_3$]$_3$ (3b): (a) Method 1. 1b (2.801 g, 1.578 mmol) dissolved in 60 mL of benzene was treated with 0.130 g (0.263 mmol) of $[(COD)RhCl]_2$ at 25 °C. After being stirred for 15 h, when a waxy, yellow precipitate was observed, the reaction mixture was treated with *c*-$C_6F_{11}CF_3$ (10 mL). The color of the fluorous phase turned to dark red, while the organic upper phase remained yellow. After phase separation the organic phase was evaporated to dryness affording a red viscous oil, which consisted of **1b** and **2b** (1:1.6 molar ratio). The fluorous phase was washed two times with 10 mL of benzene and all volatiles were removed in vacuo (0.1 bar). Further drying of the remaining dark red oil in high vacuum (10^{-6} bar) for 12 h yielded 2.497 g (0.457 mmol, 86.9% based on Rh) of a highly viscous dark red oil being pure **3b**.

(b) Method 2. 1b (0.914 g, 0.515 mmol) and 0.158 g (0.171 mmol) of $RhCl(PPh_3)_3$ were dissolved in 20 mL of benzene at 25 °C. Instantly a dark red oil precipitated. *c*-$CF_3C_6F_{11}$ (2.5 mL) was added when the formation of a dark red bottom layer and an orange upper layer was observed. The upper layer was decanted and all volatiles of the lower layer were removed in vacuo. The remaining red oil was further dried in high vacuum (10^{-6} bar, 12 h). A highly viscous dark red oil (0.690 g) containing 0.119 mmol of **3b** (69.6% based on Rh) and 0.15 equiv of **1b** was obtained. **2b** ^1H NMR (300 MHz, C_6D_6): δ 7.95 (m, 6 H, *o*-H, Si-C_6H_4), 7.24 (m, 6 H, *m*-H, Si-C_6H_4), 5.96 (s, 2 H, COD), 3.29 (s, 2 H, COD), 2.20 (m, 4 H, COD), 1.68 (dm, 4 H, COD), 1.88 (m, 6 H, CH_2CF_2), 0.81 (m, 6 H, CH_2Si), 0.01 (s, 18 H, Me). **3b**: $C_{162}H_{126}F_{153}ClSi_9P_3Rh$: calcd C 35.61, H 2.32, F 53.20, Si 4.63, P 1.70; found C 35.74, H 2.37, F 53.03, Si 4.66, P 1.65. ^1H NMR (300 MHz, $CF_3C_6F_{11}/C_6D_{14}$, 1:1 (v/v)): δ 7.43 (m, 18 H, *o*-H, Si-C_6H_4), 7.00 (m, 18 H, *m*-H, Si-C_6H_4), 1.89 (m, 18 H, CH_2CF_2), 0.85 (m, 18 H, CH_2Si), 0.15 (m, 54 H, Me). $^{13}C\{^1H\}$ NMR (75.5 MHz, $CF_3C_6F_{11}/C_6D_{14}$, 1:1 (v/v)): δ 138.7, 138.4, 137.0, 135.3, 134.7, 132.4, 128.7, 126−102 (m, CF_3, CF_2), 26.4 (t, $^2J_{C,F} = 23.8$ Hz, CH_2CF_2), 5.51 (s, CH_2Si), −4.35 (s, $^1J_{C,Si} = 52.6$ Hz, Me).

Preparation of (COD)RhCl[P(C_6H_4-*p*-$SiMe_3$)$_3$] (2c) and RhCl-[P(C_6H_4-*p*-$SiMe_3$)$_3$]$_3$ (3c). 1c (1.436 g, 2.999 mmol) and 0.177 g (0.359 mmol) of $[(COD)RhCl]_2$ were dissolved in 20 mL of *n*-hexane and 5 mL of toluene. After the mixture was stirred for 15 h all volatiles were removed in vacuo. The orange residue was dissolved in 10 mL of *n*-hexane, while the mixture was warmed up to ∼40 °C. The solution was stored at −10 °C for 12 h. The precipitate mainly consisting of **2c** was filtered off and the solution was stored for 3 days at −10 °C. Again, the precipitate was filtered off and all volatiles of the solution were removed in vacuo. **3c** (0.657 g, 0.417 mmol, 58.1% based on Rh) was obtained as an orange solid. **2c**. ^1H NMR (300 MHz, C_6D_6): δ 7.99 (m, 6 H, *o*-H, Si-C_6H_4), 7.35 (m, 6 H, *m*-H, Si-C_6H_4), 5.96 (s, 2 H, COD), 3.38 (s, 2 H, COD), 2.19 (m, 4 H, COD), 1.66 (dm, 4 H, COD), 0.13 (s, 27 H, Me). **3c**: $C_{81}H_{117}ClSi_9P_3Rh$: calcd C 61.78, H 7.49, Si 16.05, P 5.90; found C 61.65, H 7.56, Si 15.83, P 5.94. ^1H NMR (200 MHz, C_6D_6): δ 7.9 (m, 18 H, *o*-H, Si-C_6H_4), 7.2 (m, 18 H, *m*-H, Si-

(19) Osborn, J. A.; Wilkinson, G. *Inorg. Synth.* **1990**, *28*, 77−79 and 88−90.

C_6H_4), 0.18 (m, 81 H, Me). $^{13}C\{^1H\}$ NMR (75.5 MHz, C_6D_6): δ 141.3, 141.0, 137.1 (m), 135.5 (m), 134.7 (d), 133.8 (d), 132.7 (m), 132.1 (d), (C_6H_4), −0.75 (s, $^1J_{C,Si}$ = 52.5 Hz, Me).

Preparation of [Rh(μ-Cl){P(C_6H_4-*p*-$SiMe_3$)$_3$}$_2$]$_2$ (4c). Single crystals of **4c** were obtained from a solution of **3c** in a biphasic system consisting of *n*-octane and *c*-$C_6F_{11}CF_3$ (1:1, v/v, T_c = 42 °C). The molecular structure of **4c** was determined by a single-crystal X-ray structure determination study.[20]

Formation of RhCl(O_2)[P{C_6H_4-*p*-$SiMe_2R$}$_3$]$_3$ (R = $(CH_2)_2(CF_2)_5CF_3$ (5a), $(CH_2)_2(CF_2)_7CF_3$ (5b), Me (5c)). NMR tube samples of complexes **3** dissolved in C_6D_6/FC-72 (1:1 (v/v) (**3a**,**b**)) and C_6D_6 (**3c**), respectively, were exposed to the air resulting in formation of complexes **5**. Complexes **3** were reformed in 3−4 days upon addition of an excess of **1**.

Formation of RhCl(H)$_2$[P{C_6H_4-*p*-$SiMe_2R$}$_3$]$_3$ (R = $(CH_2)_2(CF_2)_5CF_3$ (6a), $(CH_2)_2(CF_2)_7CF_3$ (6b), Me (6c)). NMR tube samples of complexes **3** in C_6D_6/FC-72 (1:1 (v/v) (**3a**,**b**)) and C_6D_6 (**3c**), respectively, were frozen (−78 °C) and the dinitrogen atmosphere was replaced by dihydrogen gas. Upon warming to room temperature within minutes a color change from red to pale yellow occurred. Analysis by ^1H and ^{31}P NMR spectroscopy indicated the complete conversion of complexes **3** to dihydrides **6**. **6c**: ^1H NMR (200 MHz, C_6D_6): δ 7.8−7.2 (m, 36 H, C_6H_4), 0.18 (m, 81 H, Me), −9.1 (br, d, 1 H, $^2J_{H,P}$ = 141 Hz, Rh-H), −16.5 (br, s, 1 H, Rh-H).

Catalytic Hydrogenation Reactions. The catalytic experiments were carried out in a 30 mL Schlenk flask, under dihydrogen atmosphere (1 bar). The catalyst was dissolved in either a hydrogen-saturated toluene or perfluoro solvent and the mixture was stirred with a magnetic stirring bar (900 rpm). The olefinic substrate was added after initial dihydrogen uptake had ceased. The dihydrogen uptake was monitored using two mineral oil filled gas burets. During the hydrogenation reactions one buret was opened to the reaction vessel while the other was recharged with dihydrogen.

(a) Recycling Experiments (3a and 3b). Only catalysts prepared through method 1 were used. Catalytic reactions were carried out under single-phase fluorous conditions in *c*-$CF_3C_6F_{11}$ (2 mL) at 80 °C. After >90% conversion (monitored by the H_2 uptake) the homogeneous reaction mixture was cooled to 0 °C and the upper organic layer was siphoned off. Between cycles the fluorous layer was kept under H_2 atmosphere. By warming the solution up to 80 °C and adding a fresh portion of 1-octene (12.74 mmol) a new cycle was started. The organic phases resulting from the first cycle were analyzed by GC and ICP-AAS.

(b) Experiments in $CF_3C_6H_5$. Catalytic reactions were carried out under single-phase conditions in $CF_3C_6H_5$ at 80 °C under atmospheric hydrogen pressure. After >90% conversion (monitored by the H_2 uptake) volatiles were distilled off and analyzed by GC. Activities (TOF) were determined for 25% conversion.

Acknowledgment. This work was supported by Elf Atochem Vlissingen B.V., U-Cat (Utrecht) and The Netherlands Foundation for Scientific Research (NWO/CW, to A.L.S.). The authors, but especially B.R., would like to dedicate this work to Prof. K.-H. Thiele, on the occasion of his 70th birthday on the 9th of March 2000.

Supporting Information Available: Crystal data and details of the structure determination, final coordinates and equivalent isotropic displacement parameters of the non-hydrogen atoms, hydrogen atom positions and isotropic displacement parameters, (an)isotropic displacement parameters, bonds distances, and bond angles for **4c** (PDF). This material is available free of charge via the Internet at http://pubs.acs.org.

JA993562V

(20) X-ray data for **4c** (molecular formula: $C_{108}H_{156}Cl_2P_4Rh_2Si_{12}$ + solvent) were collected on an Enraf Nonius CAD-4T/Rotating Anode diffractometer (Mo Kα, λ = 0.71073 Å, T = 200 K) for an orange needle shaped crystal mounted with the inert oil technique at the end of an open Lindemann glass capillary. Crystal quality was limited as indicated by relatively broad, structured reflection profiles and very limited diffracted intensity beyond θ = 20°. Crystals are monoclinic, space group *C*2/*c* with cell dimensions a = 39.60(2) Å, b = 13.39(2) Å, c = 31.00(2) Å, β = 127.72(8)°, V = 13002(26) Å^3, Z = 4. A total of 11060 reflections up to θ = 20° were scanned and averaged into a unique set of 6046 reflections (of which 3806 had $I > 2\sigma(I)$). The structure was solved by standard Patterson techniques using the program *DIRDIF-96*[21] and refined on F^2 with *SHELXL97*.[22] The crystal structure was found to contain four sites filled with disordered solvent of unreliable composition. The contribution of the scattering power of the disordered solvent in that area to the structure factors was taken into account using the *BYPASS* procedure[23] as implemented as the *SQUEEZE* option in the program *PLATON*.[24] A total density equivalent with the scattering of 50 electrons per solvent accessible void of 317 Å^3 was found. Hydrogen atoms were taken into account at calculated positions and refined riding on their carrier atoms. Convergence was reached at R = 0.0745, $wR2$ = 0.187, S = 1.01, $1/w = \sigma^2(F_{obs}^2) + (0.0808P)^2$. No residual electron density was found in a final difference map outside the range $-0.84 < \Delta\rho < 0.68$ electron/Å^3. The trimethylsilyl moieties show relatively high librational motion as illustrated in the *ORTEP* Figure 2. Geometrical calculations and the *ORTEP* illustration were done with *PLATON*[24].

(21) Beurskens, P. T.; Admiraal, G.; Beurskens, G.; Bosman, W. P.; Garcia-Granda, S.; Gould, R. O.; Smits, J. M. M.; Smykalla, C. *The DIRDIF96 program system*; Technical Report of the Crystallography Laboratory; University of Nijmegen, The Netherlands, 1996.

(22) Sheldrick, G. M. *SHELXL97*; Program for crystal structure refinement; University of Göttingen: Göttingen, Germany, 1997.

(23) Van der Sluis, P.; Spek, A. L. *Acta Crystallogr*. **1990**, *A46*, 194.

(24) Spek, A. L. *Acta Crystallogr*. **1990**, *A46*, C-34.